
JOURNAL OF THE AMERICAN CHEMICAL SOCIETY

A Novel Bicyclic Enzyme Inhibitor as a Consensus Peptidomimetic for the Receptor-Bound Conformations of 12 Peptidic Inhibitors of HIV-1 Protease

Robert C. Reid, Darren R. March, Michael J. Dooley, Doug A. Bergman, Giovanni Abbenante, and David P. Fairlie*

Contribution from the Centre for Drug Design and Development, University of Queensland, Brisbane, Queensland 4072, Australia

Received February 9, 1996[®]

Abstract: The X-ray crystal structures of 12 substrate-based peptidic inhibitors bound in the active site of the aspartyl protease, HIV-1 protease, have been compared. The inhibitor-binding modes of these inhibitors are remarkably similar despite their structural diversity and conformational flexibility. This prompted the design of a bicyclic peptidomimetic inhibitor **13** with macrocyclic components in constrained conformations that are preorganized for receptor-binding. This inhibitor is a consensus conformational mimic of the protease-bound inhibitor structures with superior properties to peptides, including stability to acid and peptidases as well as antiviral activity. Each of its 15- and 16-membered rings, formed through side-chain to backbone condensation, contains two proteolytically resistant amide bonds and either isoleucine or valine linked via a short aliphatic spacer to tyrosine. The two cycles are connected by a hydroxyethylamine transition state isostere. Molecular modeling and NMR studies indicate that each macrocycle is a highly constrained structural mimic of tripeptide components of linear peptide substrates/inhibitors of HIV-1 protease. Thus the bicyclic peptidomimetic superimposes upon and structurally mimics acyclic hexapeptide inhibitors and their analogues. This results in functional mimicry, as demonstrated by comparable inhibition of HIV-1 protease by acyclic and cyclic molecules at nanomolar concentrations. The rational design of cycles which fix receptor-bound conformations of these bioactive peptides has potential applications for the structural mimicry of other bioactive peptides and may facilitate rational drug design.

Introduction

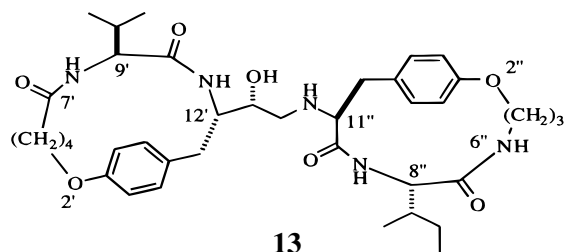
Numerous substrate-based peptidic or peptidomimetic inhibitors are now known for HIV-1 protease,¹ a critical enzyme for lytic replication of the human immunodeficiency virus type 1 (HIV-1).² Many peptidic molecules that inhibit HIV-1 protease do not prevent replication of HIV-1 in cell culture due to poor membrane penetration or proteolytic degradation by cellular

peptidases. Indeed peptidic inhibitors of enzymes generally are susceptible to proteolytic degradation by peptidases in the gut, plasma, or cells and their conformational flexibility often results in nonselective protein binding and toxicities. Other problems *in vivo* include poor oral bioavailability, inappropriate pharmacokinetics, and acquired viral resistance. Although nonpeptidic enzyme inhibitors with better *in vivo* properties than peptides have now been developed for the specific target HIV-1 protease,¹ including three inhibitors that are now licensed to treat HIV-1 infection,^{1d} there is a more general need for rational design approaches to rapidly produce enzyme inhibitors with superior properties to peptides.

The goal of this work was to rationally design a tight-binding

[®] Abstract published in *Advance ACS Abstracts*, August 1, 1996.
(1) (a) Tomasselli, A. G.; Howe, W. J.; Sawyer, T. K.; Wlodawer, A.; Heinrikson, R. L. *Chim. Oggi* **1992**, 6–27. (b) Darke, P. L.; Huff, J. R. *Adv. Pharmacol.* **1994**, 25, 399–454. (c) West, M. L.; Fairlie, D. P. *Trends Pharmacol. Sci.* **1995**, 16, 67–75. (d) March, D. R.; Fairlie, D. P. In *Designing New Antiviral Drugs for AIDS: HIV-1 Protease and Its Inhibitors*; Wise, R., Ed.; R. G. Landes Publishers: Austin, TX, 1996; p 1.

enzyme inhibitor, with higher proteolytic stability and less conformational flexibility than peptides, based upon the enzyme-bound structures of substrate-derived peptidic inhibitors. Because of the availability of X-ray crystal structural coordinates for a series of complexes between HIV-1 protease and its inhibitors (e.g., **1–12**, Table 1),^{3–14} we have chosen this system to test a general design approach to enzyme inhibitors. Here we describe a consensus peptidomimetic molecule **13**, based upon known protease-bound conformations of the 12 substrate-based peptidic inhibitors. The two macrocycles in **13** are (a)



preorganized for interaction with HIV-1 protease, (b) less conformationally flexible than acyclic components of peptidomimetic inhibitors, (c) more resistant to proteolysis than their acyclic analogues, (d) responsible in combination for potent inhibition of HIV-1 protease, and (e) sufficiently lipophilic to penetrate cell membranes for antiviral activity, whereas acyclic peptide analogues do not inhibit HIV-1 replication in cells.

(2) (a) Kohl, N. E.; Emini, E. A.; Schleif, W. A.; Davis, L. J.; Heimbach, J. C.; Dixon, R. A. F.; Scolnick, E. M.; Sigal, I. S. *Proc. Natl. Acad. Sci. U.S.A.* **1988**, *85*, 4686–4690. (b) Ashorn, P.; McQuade, T. J.; Thaisrivongs, S.; Tomaselli, A. G.; Tarpley, W. G.; Moss, B. *Proc. Natl. Acad. Sci. U.S.A.* **1990**, *87*, 7472–7476.

(3) For a review of crystallographic features of HIV-1 protease and inhibitors, see: Wlodawer, A.; Erickson, J. W. *Ann. Rev. Biochem.* **1993**, *62*, 543–585.

(4) X-ray crystal structure of **1** (pdb accession code : 1aaq): Dreyer, G. B.; Lambert, D. M.; Meek, T. D.; Carr, T. J.; Tomaszek, T. A.; Fernandez, A. V.; Bartus, H.; Cacciavillani, E.; Hassel, A. M.; Minnich, M.; Petteway, S. R.; Metcalf, B. W. *Biochemistry* **1992**, *31*, 6646.

(5) X-ray crystal structure of **2** (pdb accession code : 1hef): Krishno, H. M.; Winborne, E. L.; Minnich, M. D.; Culp, J. S.; Debouck, C. *J. Biol. Chem.* **1992**, *267*, 22770.

(6) X-ray crystal structure of **3** (pdb accession code : 1hiv): Thonki, N.; Rao, J. K. M.; Foundling, S. I.; Howe, W. J.; Tomaselli, A. G.; Heinrichson, R. L.; Thaisrivongs, S.; Wlodawer, A. To be published.

(7) X-ray crystal structure of **4** (pdb accession code : 1hvi) and of **9** (pdb accession code : 1hvj): Hosur, M. V.; Bhat, T. N.; Kempf, D.; Baldwin, E. T.; Liu, B.; Gulnik, S.; Wideburg, N. E.; Norbeck, D. W.; Appelt, K.; Erickson, J. W. *J. Am. Chem. Soc.* **1994**, *116*, 847.

(8) X-ray crystal structure of **5** (pdb accession code : 4hvp): Miller, M.; Schneider, J.; Sathyanarayana, B. K.; Toth, M. V.; Marshall, G. R.; Clawson, L.; Salk, L.; Kent, S. B. H.; Wlodawer, A. *Science* **1989**, *246*, 1149.

(9) X-ray crystal structure of **6** (pdb accession code : 8hvp): Jaskolski, M.; Tomaselli, A. G.; Sawyer, T. K.; Staples, D. G.; Heinrichson, R. L.; Schneider, J.; Kent, S. B. H.; Wlodawer, A. *Biochemistry* **1991**, *30*, 1600.

(10) X-ray crystal structure of **7** (pdb accession code : 9hvp): Erickson, J.; Neidhart, D. J.; Van Drie, J.; Kempf, D. J.; Wang, X. C.; Norbeck, D. W.; Plattner, J. J.; Rittenhouse, J. W.; Turon, M.; Wideburg, N.; Kohlbrenner, W. E.; Simer, R.; Welfrich, R.; Paul, D. A.; Knigge, M. *Science* **1990**, *249*, 527.

(11) X-ray crystal structure of **8** (pdb accession code : 1hps): Thompson, S. K.; Murthy, K. H. M.; Zhao, B.; Winborne, E.; Green, D. W.; Fisher, S.; DesJarlais, R. L.; Tomasek, T. A.; Meek, T. D.; Gleeson, J. G.; Abdel-Meguid, S. S. To be published.

(12) X-ray crystal structure of **10** (pdb accession code : 4phv): Bone, R.; Vacca, J. P.; Anderson, P. S.; Holloway, M. K. *J. Am. Chem. Soc.* **1991**, *113*, 9382.

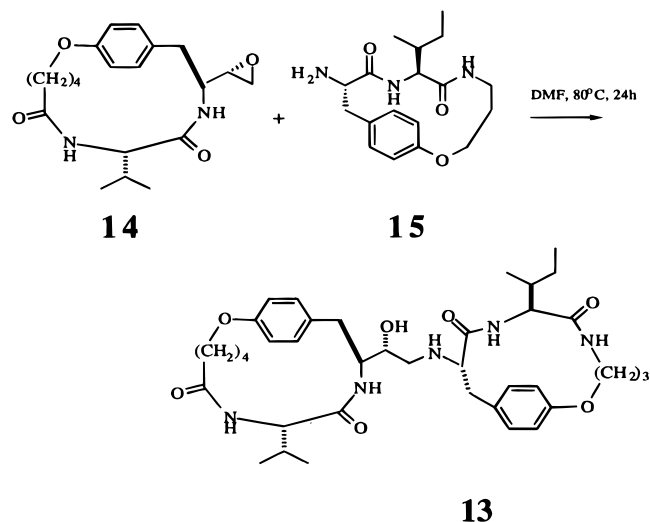
(13) X-ray crystal structure of **11** (pdb accession code : 1sbg): Abdet Meguid, S. S.; Metcalf, B. W.; Carr, S. T. J.; Demarsh, P.; DesJarlais, R. L.; Fisher, S.; Green, D. A.; Ivonoff, L.; Lambert, D. M.; Murthy, K. H. M.; Petteway, S. R.; Pitts, W. J.; Tomasek, T. A.; Winborne, E.; Zhao, B.; Dreyer, G. B.; Meek, T. D. To be published.

(14) X-ray crystal structure of **12** (pdb accession code : 7hvp): Swain, A.; Miller, M. M.; Green, J.; Rich, D. H.; Schneider, J.; Kent, S. B. H.; Wlodawer, A. *Proc. Natl. Acad. Sci. U.S.A.* **1990**, *87*, 8805–8809.

Results and Discussion

Design and Synthesis. The three-dimensional structures^{4–14} of 12 substrate-based enzyme-bound peptidic inhibitors of HIV-1 protease (Table 1) are shown overlaid in Figure 1a. This range of inhibitors includes MVT101 (**5**) and JG365 (**12**), which do not exhibit antiviral activity in cell culture, and SKF108738 (**2**), U75875 (**3**), A77003 (**4**), and SB206343 (**8**) and (**10**) which are antiviral *in vitro* but did not advance to the clinic due to other problems. On the basis of the common regions in Figure 1a, we designed the bicyclic compound **13** as a consensus structure, shown by its accurate superposition on the other 12 structures (Figure 1b). This particular bicycle consists of two similar macrocycles, formed by linking the oxygens of tyrosine side chains with main chain amides.

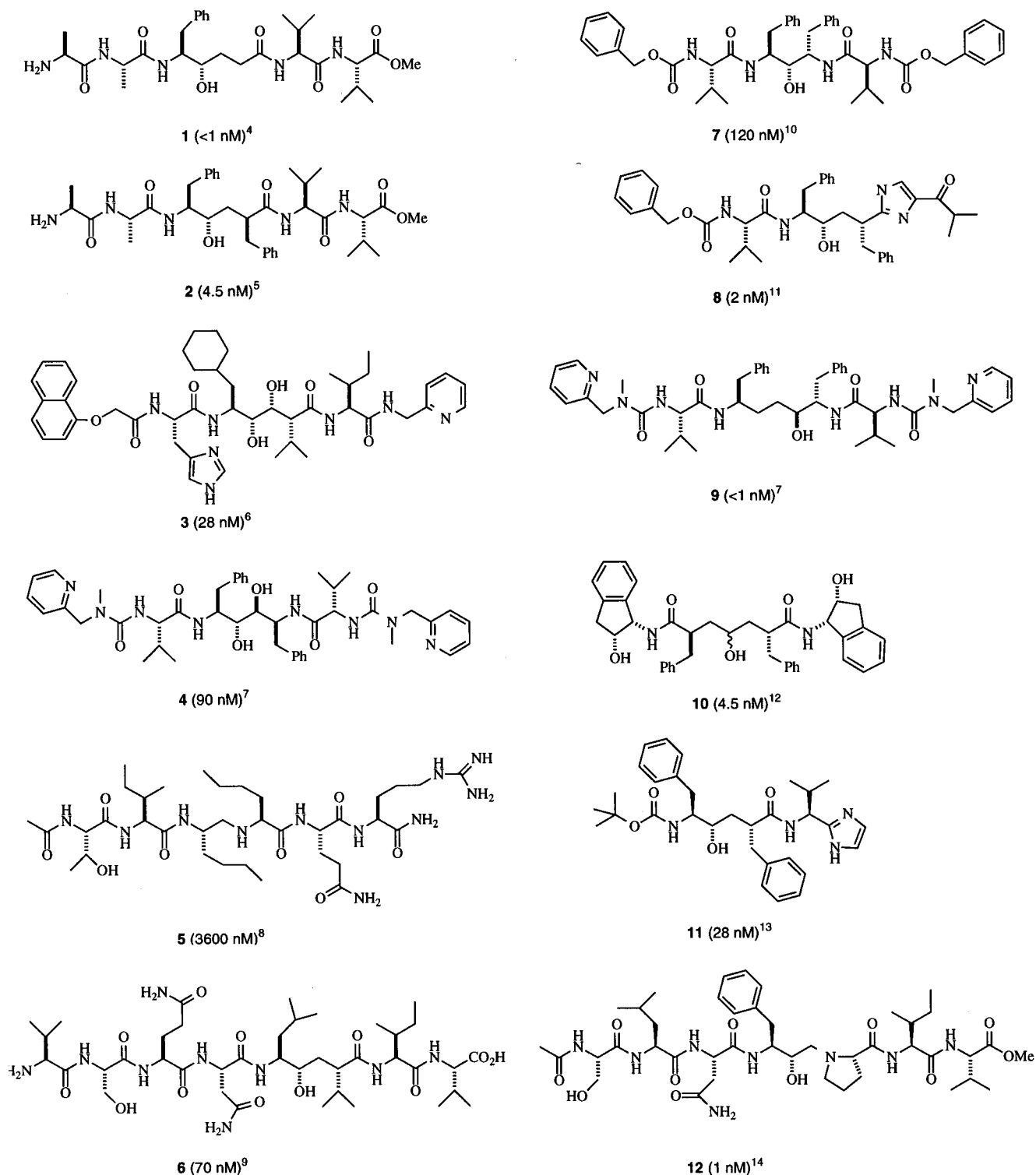
Although **13** has six chiral centers, its synthesis is relatively straightforward because five of the chiral centers are derived simply from L-amino acids and the sixth is readily controlled via a diastereoselective^{15a} synthesis involving the chiral (*2S*)-epoxide intermediate^{15b} **14**. Compound **13** was prepared in solution by coupling its component halves **14** and **15** and characterized by 2D-NMR (¹H, ¹³C) spectroscopy and mass spectrometry. We have previously reported^{16,17} the synthesis of compounds containing one or other of the cycles in **13**.



Conformational Restrictions. It was not possible to determine the three-dimensional solution structure of **13** by 2D NMR spectroscopy because of the lack of long range NOE data. However 1D ¹H-NMR spectra in CD₃OH for each of its composite monocycles in other compounds¹⁶ show four distinct aromatic proton resonances for each cycle, indicative of restricted rotation of the phenyl ring. Also bicycle **13** in CD₃-OH at 300 K shows distinct ¹H NMR resonances (1D and Cosy) for each of the eight aromatic protons belonging to the tyrosine-derived aromatic rings, consistent with restricted rotation for both aromatic rings. At this temperature, signals for the larger N-terminal cycle were clearly closer to coalescence than those for the smaller C-terminal cycle. Variable temperature ¹H-NMR experiments in DMSO-*d*₆ (not shown) led to coalescence at ~330 K to two signals of resonances attributed to the the larger

(15) (a) Epoxides: Rich, D. H.; Sun, C.-Q.; Prasad, J. V. N. V.; Pathiasseril, A.; Toth, M. V.; Marshall, G. R.; Clare, M.; Mueller, R. A.; Houseman, K. *J. Med. Chem.* **1991**, *34*, 1222–1225. (b) The synthesis of **14** (shown in Scheme 1, supporting information) and the *S*-diastereomer of **13** are described in detail elsewhere: Reid, R. C. et al Submitted for publication.

(16) Abbenante, G.; March, D. R.; Bergman, D. A.; Hunt, P. A.; Garnham, B.; Dancer, R. J.; Martin, J. L.; Fairlie, D. P. *J. Am. Chem. Soc.* **1995**, *117*, 10220–10226.

Table 1. Structures of Twelve Peptidic Inhibitors of HIV-1 Protease (K_i)

N-terminal macrocycle, suggesting that free rotation of the aromatic ring is occurring at the higher temperature. On the other hand, the four remaining aromatic proton resonances for the smaller C-terminal cycle of **13** persisted even at 400 K (upper limit for experiments), implying highly restricted rotation. These observations are consistent with limited conformational freedom for both macrocyclic components of **13** at physiologically relevant temperatures.

Further support for limited conformational flexibility in each cycle comes from molecular modeling studies of **13**. A Dreiding model of **13** reveals that the short aliphatic spacer in each macrocyclic component only just connects the planar aromatic

ring to the rigid region containing the two amide planes. Using computer modeling, unrestrained molecular dynamics on the bicycle led to the superimposed images in Figure 2a,b, each of which shows 200 dynamics frames saved at 1 ps intervals and energy minimized. All carbon, nitrogen, and oxygen atoms of the N-terminal cycle superimpose to rmsd's <0.3 Å (Figure 2a), while the same atoms of the C-terminal cycle superimpose to rmsd's <0.7 Å (Figure 2b). The dynamics trajectory clearly illustrates the constrained nature of each monocycle—the aromatic ring, two amide bonds, and Val/Ile side chain being virtually locked into position.

Although each cyclic component of **13** is conformationally

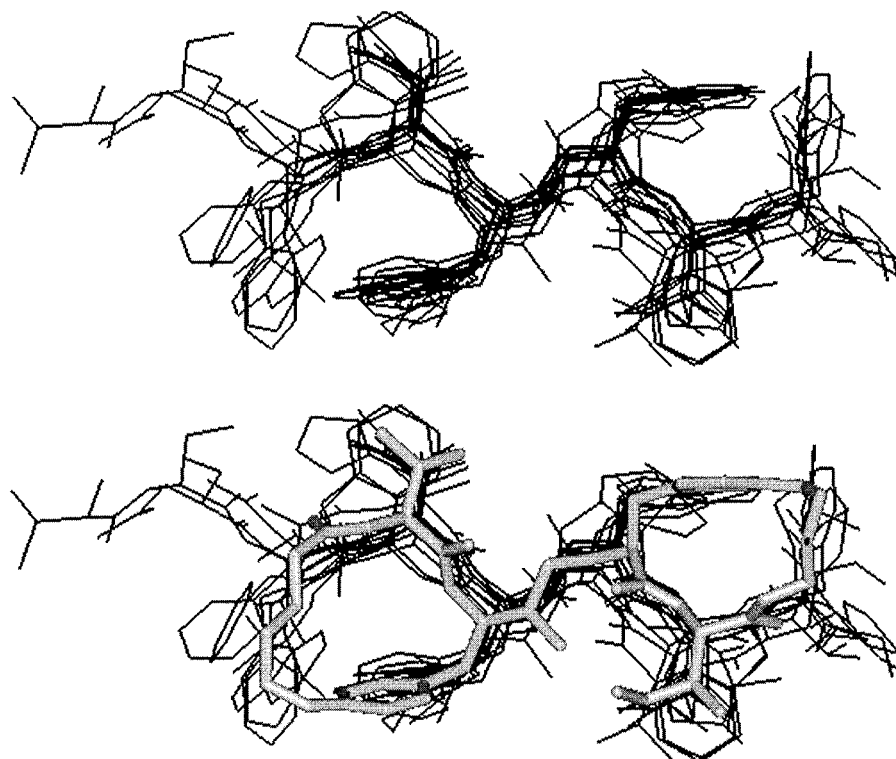
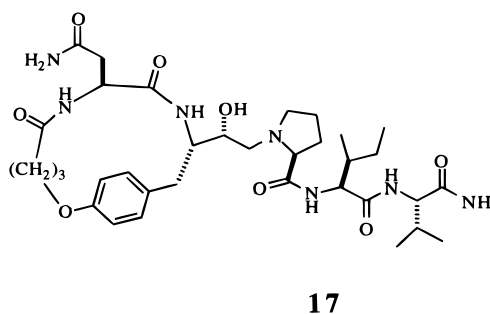
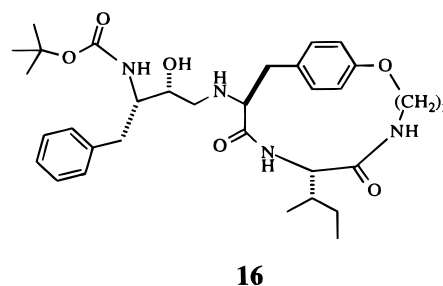


Figure 1. (a, top) Superimposed structures of the receptor-bound conformations of 12 peptidomimetic inhibitors of HIV-1 protease (see Table 1) taken from X-ray crystal structures of their complexes with HIVPR⁴⁻¹⁴. (b, bottom) Energy minimized modeled¹⁸ structure of **13** (grey) in the putative HIVPR-binding conformation overlaid upon the 12 crystallographic structures shown in (a).

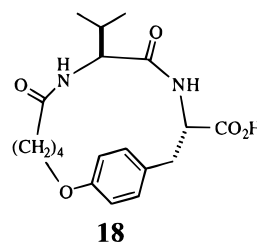
rigid, the bicycle possesses some conformational freedom as a result of each cycle being able to rotate relative to the other about the linking transition state isostere (Figure 2). The bicycle might be further conformationally constrained if additional bulk were incorporated into this isostere (e.g., an NET substituent). Nevertheless examination of all available HIV-1 protease structures, including those in Figure 1, clearly reveals that only one conformation (the extended conformation) is recognized by the enzyme. In summary, the cyclic components of the bicycle impart significant conformational rigidity to >90% (47 of the 51 heavy atoms) of the molecule, making it significantly more conformationally constrained than acyclic hexapeptides.

Although we have been unable to suitably crystallize **13** for X-ray structural investigation, we have recently reported the X-ray structures of compounds **16** and **17**, containing N- and C-terminal cycles, bound to HIV-1 protease.^{16,17} For those solid-state structures, the C-terminal cycle of **16** and the N-terminal cycle of **17** precisely superimposed upon the protease-bound conformations of acyclic peptides. This strongly supports our assertion that the individual cycles in **13** are conformationally preorganized for receptor-binding.

Biological Properties. The structural mimicry, evident in the above modeling studies for **13** and in X-ray crystal structures of the separate monocycles **16** and **17** of which **13** is composed, correlates with functional mimicry. For example, **13** (IC₅₀ 5 nM) was equipotent with its linear hexapeptide analogue Ac-Leu-Val-Phe-{CHOHCH₂N}-Phe-Ile-Val-NH₂ (IC₅₀ 5 nM) in inhibiting HIV-1 protease.¹⁹ The *S*-diastereomeric alcohol of **13** is a ~20 fold less potent inhibitor^{15b} than the *R*-diastereomer. This finding is supported by molecular modeling¹⁸ of the two diastereomers, the *R*-isomer superimposes more accurately upon



the putative protease-bound conformation^{16,17} of a hexapeptide analogue Ac-Leu-Val-Phe-{*CHOHCH₂N}-Phe-Ile-Val-NH₂.



(17) March, D. R.; Abbenante, G.; Bergman, D. A.; Brinkworth, R. I.; Wickramasinghe, W. A.; Begun, J. J.; Martin, J. L.; Fairlie, D. P. *J. Am. Chem. Soc.* **1996**, *118*, 3375–3379.

(18) Insight 2.3.5 and Discover 2.9.6 (Biosym Technologies, San Diego) were used on a Silicon Graphics Extreme work station.

To gauge the contribution that each monocycle makes to the activity of the bicycle we tested the inhibitor potency of **15**

and **18** against HIV-1 protease. Neither compound was a potent inhibitor ($IC_{50} \sim 15$ and $\sim 8 \mu M$, respectively) in contrast to the bicycle **13** ($IC_{50} 5$ nM). Together with other data for compounds containing these cycles^{16,17} it is evident that like tripeptides, which they mimic, additional interactions need to be made with the enzyme to obtain potency and selectivity at nM concentrations of inhibitor.

By conformationally constraining the two otherwise flexible tripeptide components to the receptor-binding cyclic conformations in **13**, a significant entropy advantage was expected for inhibitor binding over the acyclic inhibitor¹⁷ Ac-Leu-Val-Phe- $\{^*CHOHCH_2N\}$ -Phe-Ile-Val-NH₂. However the latter makes H-bonds from the acetyl, terminal Leu-CO, and Val-CONH₂ to the enzyme which cannot be made by the cycles of **13**. H-bonding from these terminal Leu/Val residues is not possible in the cycles of **13**, as shown by X-ray structures of the individual cycles in other inhibitors,^{16,17} due to twisting of the amide out of the extended conformation recognized by the protease. Despite this loss of potential hydrogen-bonding interactions as well as some residual rotational freedom about the transition state isostere (Figure 2), the bicyclic inhibitor **13** must gain some entropy advantage over the conformationally more flexible acyclic inhibitor since it is equipotent as an inhibitor of HIV-1 protease.

Constricting the tripeptide sequences into macrocycles^{16,17} was also expected to make the amide bonds less recognizable to other proteases, which degrade the acyclic peptide, and hence more resistant to cleavage. This expectation has been realized, each of the cycles in **13** being stable to hydrolysis by 3 M HCl, gastric peptidases, and human plasma.²⁰ As a consequence of having enhanced stability to proteolytic cleavage and appropriate lipophilicity,^{21a} the bicyclic compound inhibits HIV-1 replication ($IC_{50} \sim 60$ nM) in cell culture unlike the more degradable acyclic peptides (e.g., JG365, MVT101) which are inactive as antiviral agents *in vitro* at 100 μM concentrations under the same testing conditions.^{21b}

Conclusions

An increasing number of natural and synthetic cyclic peptides are being identified as potent regulators of biological processes.²³ To date such structures have been optimized for activity through random changes which have met with limited success in the development of bioactive peptides.²³ However, this work suggests that directly mimicking the receptor-binding conformations of peptides holds promise for rational design of functional peptidomimetics. The specific application here to the design and development of an inhibitor of the proteolytic enzyme

(19) Enzyme/assay references: (a) Schneider, J.; Kent, S. B. H. *Cell* **1988**, *54*, 363–8. (b) Wlodawer, A.; Miller, M.; Jaskólski, M.; Sathyanarayana, B. K.; Baldwin, E.; Weber, I. T.; Selk, L. M.; Clawson, L.; Schneider, J.; Kent, S. B. H. *Science* **1989**, *245*, 616–621. (c) Bergman, D. A.; Alewood, D.; Alewood, P. F.; Andrews, J. L.; Brinkworth, R. I.; Engelbrechtsen, D. R.; Kent, S. B. H. *Lett. Peptide Sci.* **1995**, *2*, 99–107.

(20) Passmore, M. et al Unpublished work. Detailed analyses of these and other cycles will be reported separately in the context of structure–activity relationships and pharmacological properties of macrocyclic inhibitors of HIV-1 protease.

(21) (a) $\log P_{(o/w)} = 2.7$ for **13**, calculated using PALLAS pKalc and PrologP available from CompuDrug Chemistry Ltd, Hungary. (b) **13** has similar antiviral activity ($EC_{50} \sim 60$ nM) to DM323²² ($EC_{50} \sim 110$ nM) when exposed for 4 days to PHA-stimulated cord blood mononuclear cells infected with HIV-1 (strain TC354). Inhibition of HIV replication was determined by RT activity, assessed 4 days post inoculation.

(22) Lam, P. Y. S.; Jadhav, P. K.; Eyermann, C. J.; Hodge, C. N.; Ru, Y.; Bachelier, L. T.; Meek, J. L.; Otto, M. J.; Rayner, M. M.; Wong, Y. N.; Chang, C.-H.; Weber, P. C.; Jackson, D. A.; Sharpe, T. R.; Erickson-Viitanen, S. *Science* **1994**, *263*, 380–384.

(23) Fairlie, D. P.; Abbenante, G.; March, D. R. *Curr. Med. Chem.* **1995**, *2*, 672–705 and references therein.

HIV-1 protease exemplifies a mimetic approach that could also be applicable to bioactive peptides that target other receptors. The novel cycles are easily synthesized, conformationally rigid, proteolytically stable, and water and lipid soluble and can be readily varied by altering the size or substituents of a cycle. Such molecules promise to be important mechanistic probes of biological processes and potential drug leads.

Experimental Section

General Methods. ¹H NMR spectra were recorded on a Bruker ARX 500 MHz NMR spectrometer using CD₃OH as an internal standard. Proton assignments were made using DQCOSY, NOESY, and TOCSY experimental data. Variable temperature experiments were conducted in CD₃OH or DMSO-*d*₆ in the range 20–130 °C. The ¹³C NMR spectrum was recorded on a Varian Gemini 300 at 75 MHz in methanol-*d*₄ and was referenced to the solvent peak at δ 49.0 ppm. Preparative scale HPLC separations were performed on Waters Delta-Pak Prep-Pak C18 40 mm \times 100 mm cartridges (100 Å) and analytical reverse phase HPLC was performed on Waters Delta-Pak Radial-Pak C18 8 mm \times 100 mm cartridges (100 Å) using gradient mixtures of water/0.1% TFA and water 10%/acetonitrile 90%/0.1% TFA.

Mass spectra were obtained on a triple quadrupole mass spectrometer (PE SCIEX API III) equipped with an Ionspray atmospheric pressure ionization source (ISMS). Solutions of compounds in 9:1 acetonitrile/0.1% aqueous trifluoroacetic acid were injected by syringe infusion pump at mM-pM concentrations and flow rate of 20–50 μL /min into the spectrometer. Molecular ions, $[M + nH]^{n+}/n$, were generated by ion evaporation and focussed into the analyzer of the spectrometer through a 100 mm sampling orifice. Full scan data was acquired by scanning quadrupole-1 from m/z 100–900 with a scan step of 0.1 dalton and a dwell time of 2 ms. Accurate mass determinations were performed on a KRATOS MS25 mass spectrometer using Electron Impact ionization.

Synthesis. The syntheses of epoxide **14**^{15b} (Scheme 1, supporting information) and amine **15**^{16,17} have been reported elsewhere, but NMR spectral data for **14** are described here for the first time.

NMR Spectra for 14: ¹H NMR (300 MHz, CD₃OH) δ 7.90 (d, $J = 9.8$ Hz, 1H, tyr NH); 7.47 (d, $J = 8.8$ Hz, 1H, val NH); 7.14 (dd, $J = 8.4, 2.2$ Hz, 1H, ArH); 7.01 (dd, $J = 8.2, 2.3$ Hz, 1H, ArH); 6.42 (dd, $J = 8.4, 2.6$ Hz, 1H, ArH); 6.77 (dd, $J = 8.2, 2.7$ Hz, 1H, ArH); 4.28–4.03 (m, 3H, tyr α H and CH₂OAr); 3.90 (t, $J = 8.8$ Hz, 1H, val α H); 3.09 (dd, $J = 13.3, 4.1$ Hz, 1H, tyr β H); 3.04 (ddd, $J = 6.5, 3.9, 2.7$ Hz, 1H, epoxide CH); 2.75 (dd, $J = 5.0, 3.9$ Hz 1H), and 2.69 (dd, $J = 5.0, 2.7$ Hz, 1H, epoxide CH₂); 2.46 (dd, $J = 13.3, 12.5$ Hz, 1H, tyr β H); 2.19–2.05 (m, 2H, –CH₂CO); 1.86–1.69 (m, 2H, val β H and –CH₂–); 1.60–1.22 (m, 3H, –CH₂CH₂–); 0.87 (d, $J = 6.7$ Hz, 3H, Val Me) and 0.83 (d, $J = 6.7$ Hz, 3H, Val Me). ¹³C NMR (DMSO-*d*₆): δ 171.23, 170.50, 154.82, 131.29, 130.71, 129.07, 118.49, 117.42, 68.06, 57.59, 53.09, 50.17, 43.48, 36.28, 34.94, 31.15, 25.82, 21.75, 18.99, 18.94.

Synthesis of [(2R),(8'S),(9'S),(11'S),(12'S)]-2-[12'-(7',10'-dioxo-9'(isopropene)-2'-oxa-8',11'-diazabicyclo[12.2.2]-octadeca-14',15',17'-triene]-1-[11'-(7'',10''-dioxo-8''-(1-methylpropyl)-2''-oxa-6'',9''-diazabicyclo[11.2.2]-heptadeca-13'',15'',16''-triene]aminoethan-2-ol **13.** The epoxide **14** (20 mg, 56 μ mol), amine **15** (75 mg, 225 μ mol), and diisopropylethylamine (10 μ L) were heated and stirred in dry DMF (500 μ L) at 80 °C for 24 h. The mixture was evaporated to dryness *in vacuo*, and the residue was dissolved in a mixture of MeCN (3 mL), water (7 mL), and trifluoroacetic acid (0.25 mL). The solution was purified by rp-HPLC on a Waters Delta-Pak cartridge (C18, 15 μ m, 100 Å, 40 \times 100 mm) using a linear gradient from (99.9% H₂O + 0.1% TFA) to (49.95% H₂O, 49.95% MeCN + 0.1% TFA) over 25 min, at a flow rate of 30 mL min⁻¹ and UV detection at 230 nm, retention time 17 min. Fractions containing the bicycle were combined and lyophilized giving a white powder (15 mg, 35%). ¹H NMR (500 MHz, CD₃OH, 300 K): δ 7.91 (d, $J = 9.5$ Hz, 1H, 11'-NH), 7.84 (dd, $J = 6.6, 3.6$ Hz, 1H, CH₂NH), 7.51 (d, $J = 9.4$ Hz, 1H, Val NH), 7.24 (d, $J = 7.6$ Hz, 1H, Ile NH), 7.13 (dd, $J = 8.4, 2.0$ Hz, 1H, 15' or 18'-CH), 7.10 (dd, $J = 8.3, 2.1$ Hz, 1H, 14' or 17'-CH), 7.02 (dd, $J = 8.2, 2.2$ Hz, 1H, 15' or 18'-CH), 6.95 (m, 1H, 14' or 17'-CH), 6.89 (m, 1H, 15' or 16'-CH), 6.86 (m, 1H, 16' or 17'-CH), 6.84 (m,

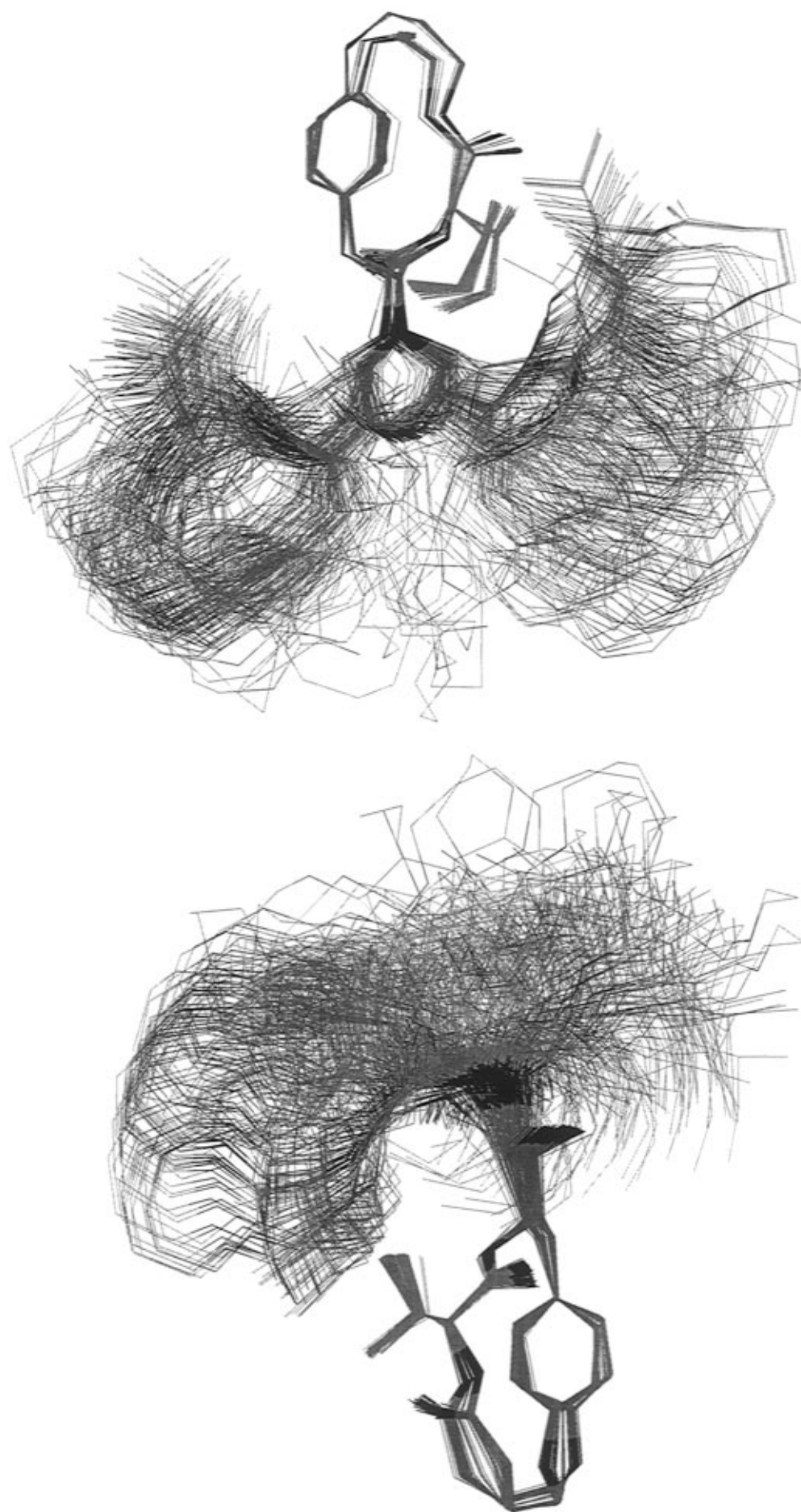


Figure 2. Molecular dynamics trajectories for bicycle **13** showing superimposition of all carbon, nitrogen, and oxygen atoms of (a, left) the N-terminal cycle and (b, right) the C-terminal cycle. Details are given in the text and Experimental Section.

¹H, 15'' or 16''-CH), 6.77 (dd, *J* = 8.2, 2.7 Hz, 1H, 16' or 18'-CH), 4.39 (m, 1H, 3''-CH₂), 4.24 (m, 1H, 3''-CH₂), 4.20 (m, 1H, 3'-CH₂), 4.15 (dd, *J* = 10.7, 6.9 Hz, 11''-CH), 4.10 (m, 1H, 3'-CH₂), 4.05 (m, 1H, 12'-CH), 3.95 (dd, *J* = 9.4, 8.4 Hz, Val αH), 3.81 (m, 1H, CHOH), 3.57 (m, 1H, 5''-CH), 3.47 (dd, *J* = 7.6, 7.0 Hz, Ile αH), 3.40 (dd, *J* = 12.2, 6.9 Hz, 12''-CH), 3.24 (dd, *J* = 13.5, 3.8 Hz, 13'-CH), 3.10 (dd, *J* = 12.4, 2.8 Hz, 1H, CHOCH₂NHR), 2.92 (dd, *J* = 12.4, 8.7 Hz, 1H, CHOCH₂NHR), 2.80 (m, 1H, 5''-CH), 2.77 (dd, *J* = 12.2, 10.7 Hz, 1H, 12''-CH), 2.40 (dd, *J* = 13.5, 12.3 Hz, 1H, 13'-CH), 2.26 (m, 1H, 4''-CH), 2.11 (m, 1H, 6'-CH), 2.10 (m, 1H, 5'-CH), 1.79 (m, 1H, Val βH), 1.76 (m, 1H, 6'-CH), 1.74 (m, 1H, 4''-CH), 1.64 (m, 1H, 4'-CH), 1.57 (m, 1H, Ile βH), 1.45 (m, 1H, 5'-CH), 1.41, (m, 1H, Ile CH₂), 1.31 (m, 1H, 4'-CH), 0.95 (m, 1H, Ile CH₂), 0.87 (d, *J* = 6.6 Hz, Val CH₃), 0.85 (t, *J* = 7.1 Hz, 3H, Ile CH₃), 0.81 (d, *J* = 6.8 Hz, 3H, Val CH₃), 0.76 (d, *J* = 6.9 Hz, 3H, Ile CH₃). ¹³C NMR (CD₃OD, 75 MHz) δ 174.99, 173.68, 171.16, 167.32, 160.20, 156.66, 132.34, 131.98, 130.51, 130.15, 127.69, 119.57, 118.87, 118.75, 70.87, 69.25, 68.58, 63.69, 59.96, 59.67, 55.84, 51.06, 39.96, 37.77, 37.65, 36.83, 36.20, 32.79, 27.57, 27.29, 26.70, 22.59, 20.16, 18.91, 14.91, 11.92. MS (electrospray): *m/z* 694 [M + H]⁺ (100%). HRMS (EI⁺) *m/e* 693.4095, M⁺ calculated for C₃₈H₅₅N₅O₇ 693.4088.

Computer Modeling. The bicyclic was built on screen using the builder module of InsightII molecular modeling system (Biosym/MSI, San Diego), and energy minimizations were carried out using Discover (version 2.9.6). Unrestrained dynamics (200 ps) was performed at 300 K with Discover using the cvff forcefield with no formal charges assigned and in a dielectric of 1. Two hundred dynamics frames were saved at 1 ps intervals and energy minimized. The heavy atoms in the N-terminal cycle of all 200 dynamics frames superimposed to rmsd's <0.3 Å with reference to the N-terminal cycle of the initial dynamics frame. Similarly, the heavy atoms of the C-terminal cycle superimposed

to rmsd's <0.7 Å with reference to the C-terminal cycle of the initial dynamics frame. The dynamics trajectories for the N-terminal cycles and C-terminal cycles superimposed are illustrated in Figure 2.

HIV-1 Protease Activity. Synthetic HIV-1 protease was prepared as described^{19a} except that Aba replaced Cys residues in the SF2 isolate as footnoted elsewhere.^{19b} **13** was assayed *in vitro* (pH 6.5, *I* = 0.1 M, 37 °C, 50 μM substrate [Abz-NF*-6]) for inhibition of the action of the synthetic HIV-1 protease using a reported fluorometric assay.^{19c}

Proteolytic Stability.²⁰ Stability of **15** and **18** were determined by (a) dissolving in 3 M HCl (45 °C, 4 days), HPLC and mass spectrometry indicated no degradation of either cycle and (b) incubating with plasma (37 °C, 1 h) from human blood (5 mL) after clotting (1 h) and centrifuging (5 min), adding acetonitrile (1 mL, 4 °C), vortexing (30 s), and centrifuging (5 min, 4 °C). The supernatant was removed, frozen in liquid N₂, lyophilized, and resuspended in 100 μL buffer, and intact cycles were detected by HPLC and electrospray mass spectrometry. No decomposition was observed: (c) after incubating with pepsin or rat gastric juice (37 °C, 1 h, pH 3), rp-HPLC and mass spectrometry showed only intact macrocycles.

Acknowledgment. The National Health and Medical Research Council and the Commonwealth AIDS Research Grant Scheme contributed some financial support and thanks go to Dianne Alewood for providing synthetic enzyme.

Supporting Information Available: Scheme 1 summarizes the synthesis of **14** (1 page). See any current masthead page for ordering and Internet access instructions.

JA960433V